Nanomedicine Journal

Received: Oct. 19, 2013; Accepted: Dec. 3, 2013
Vol. 1, No. 3, Spring 2014, page 162-170

Online ISSN 2322-5904
http://nmj.mums.ac.ir

Original Research

Discovery of active site of vinblastine as application of nanotechnology in medicine

Zahra Varmaghani[1*], Majid Monajjemi[2], Fatemeh Mollaamin[3]

[1]Department of Biology, Science and Research Branch, Islamic Azad University, Tehran, Iran
[2]Department of Chemistry, Science and Research Branch, Islamic Azad University, Tehran, Iran
[3]Department of Chemistry, Qom Branch, Islamic Azad University, Qom, Iran

Abstract

Objective(s): Vinblastine is antimitotic, anticancer medicine that disturbs normal microtubule formation and favours depolymerisation. Structural study and finding the active site of vinblastine are the targets of this research.
Materials and Methods: Vinblastine was optimized in vacuum and then in different solvents by Density Functional Theory (DFT) method. Nuclear Magnetic Resonance (NMR) shift measurements were made in different solvents by various dielectric constants by Continuous Set of Gauge Transformations (CSGT).
Results: The best structure and function of vinblastine was established. The conformational preferences may be attributed to stereoelectronic effects. The results showed that the structure of vinblastine is more stabile in water rather than the other media. The most active atoms of vinblastine were realized by various spectra of vinblastine in different media including vacuum and diverse solvents.
Conclusion: Discovery of active site of vinblastine that could bind to tubulin to perform the antimitosis and anticancer effect in process of cell division was accomplished in this investigation. These data can be applicable to study the binding site of vinblastine-tubulin complex.

Keywords: Anticancer, Density functional theory, Nanosystem,Vinblastine

***Corresponding author:** Zahra varmaghani, Department of Biology, Science and Research Branch, Islamic Azad University, Tehran, Iran.
Tel: +982147912396, Email: z_varmaghani@yahoo.com*

Introduction

Molecular modeling and quantum mechanical simulations using the density functional theory play an increasingly important role in fundamental understanding of nanoscale phenomena and as well as in technological applications. Nanotechnology is the study of manipulating matter on an atomic and molecular scale to develop materials, devices and other structures at a scale of 1 to 100 nanometers. Approaches of atomic-scale computer modeling can be applied to large molecules of technological interest, supramolecular structures in interaction, or adsorbed at surfaces, and bulk systems for which nanostructural units can be clearly identified.

We concentrate on the characterization of nanosystems (vinblastine among different solvent molecules) at the atomic scale by quantum mechanical simulations using the density functional theory.

Biologically processes of medicinal chemistry depend on many other disciplines ranging from organic chemistry and pharmacology to computational chemistry.

Typically medicinal chemists use the most straight forward ways to prepare compounds. The validation of any design project comes from the biological testing. Cancer is a general term used to describe a disease state that is characterized by abnormal cell proliferation. The causes which bring about this abnormal cellular behaviour are specific to each type of cancer (1-5).

Vinblastine causes mitotic arrest by interacting with tubulin heterodimers and mitotic spindle microtubules, and so this medicine inhibits the polymerization of tubulin into microtubules by acting at the ends of microtubules and diminishes an essential aspect of cell division, dynamic instability. Vinblastine produces its antitumor effects by halting cell division at metaphase. Vinblastine has two moieties (catharanthine and vindoline moieties), that the catharanthine moiety (Figure 1) affects tubulin spiraling. Vindoline moiety is important in anchoring the drug molecule. This drug interacts in vivo with free tubulin and tubulin in mitotic spindles causing spiral formation and diminishes microtubules dynamic instability (6-9). The importance of vinblastine has motivated us to analyze the optimized nanosystem of vinblastine among solvent molecules and finding the active site of vinblastine for binding to tubulin using theoretical methods.

The results indicate good agreement in all of the methods.

There are further molecules that play role in binding vinblastine to tubulin. These molecules are bounded to vinblastine-tubulin complex to make a supracomplex. Recognizing the most active site of each molecule seems to be important to study this supracomplex. Discovery the active site of these molecules would be performed by quantum mechanical simulations using DFT method.

In this paper we have investigated on the most active atoms of vinblastine. Therefore, these atoms are more important in binding to tubulin rather than the other atoms.

Discovery the best optimized structure such as bond lengths, bond angles, dihedral angles and total atomic charges and finding the most active atoms, and then the effect of different dielectric constants on that could use to make the best structure of vinblastine that its affinity for tubulin could be high and act the most effective interactions with tubulin and do the best function in therapy of cancer.

This could be a result in medicinal chemistry field that was not easily obtained without using modelling and simul-ation.

Device modeling and simulation are

important aspects of this work. These are necessary in making predictions before experiments are done, as well as interpreting the data after experiments.

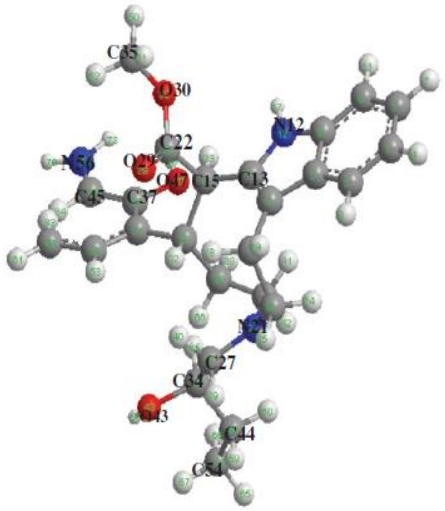

Figure 1. Catharanthine moiety of vinblastine.

Theoretical methods

Biologically processes also occur in aqueous solution systems with rather specific pH and ionic conditions. Most reactions are both qualitatively and quantitatively different under vacuum and solution phase conditions, especially those involving ions or polar species. Molecular properties are also sensitive to the environment. Simulations are therefore intimately related with describing solute-solvent interactions, but such effects can also be modelled with less rigorous methods. In this research the vinblastine was optimized by hybrid density functional theory (B3LYP) and hartree–Fock (HF) (10-13) methods using sto-3g, 3-21g and 6-31g basis sets. A basis set in theoretical and computational chemistry is a set of functions. These functions are typically atomic orbitals cantered on atoms. When molecular calculations are performed, it is common to use a basis composed of a finite number of atomic orbitals, centered at each atomic nucleus within the molecule. Sto-3g, 3-21g and 6-31g describe the type of atomic orbitals, for example Slater-type orbitals (STOs). Sto-3g basis set calculates superficial orbitals on atoms, whereas 3-21g and 6-31g basis sets estimate central orbitals. The greater number of basis set, the more central orbital.

NMR chemical shift

The chemical shift refers to the phenomenon which is associated with the secondary magnetic field created by the induced motions of the electrons. The energy of a magnetic moment, μ, in a magnetic field, B, is as follow:

$$E = -\mu . (1 - \sigma) B \quad [1]$$

Where the shielding σ, is the differential resonance shift due to the induced motion of the electrons. The chemical shielding is characterized by a real three-by-three Cartesian matrix (14). For brevity, these values are usually referred to shielding tensor:

$$\begin{bmatrix} \sigma xx & \sigma xy & \sigma xz \\ \sigma yx & \sigma yy & \sigma yz \\ \sigma zx & \sigma zy & \sigma zz \end{bmatrix} \quad [2]$$

The isotropic value (σ) of the shielding tensor is defined as

$$\sigma iso = 0.33(\sigma 11 + \sigma 22 + \sigma 33) \quad [3]$$

The anisotropy (Δσ) of the tensor and shielding tensor asymmetry parameter (η) are determined according to Eq. 4 and 5, respectively.

$$\Delta\sigma = \sigma 33 - 0.5(\sigma 11 + \sigma 22) \quad [4]$$

$$\eta = \frac{\left| \sigma 22 - \sigma 11 \right|}{\left| \sigma 33 - \sigma iso \right|} \quad [5]$$

The electronic structure plays a primary role in determining structure of a molecule. To test the influence of the polarized continuum on molecular structure the geometry optimizations were made in water, methanol and ethanol using self-consistent reaction field (SCRF = dipole) by Gaussian 98 program.

The computations refer to vinblastine molecule, unpolarized by any solvent molecules, whereas the (NMR) shift measurements were made in water,

methanol and ethanol solvents with various dielectric constants, (78.39, 32.63 and 24.55, respectively).

Results and Discussion

Defining the relationship between the dielectric constant, the geometrical structure and the optimized energy is central to understanding the mechanism of dynamic modeling by a few force field of simulation. The results of calculations have represented with the Onsager model.

The comparison of vinblastine structure between vacuum and water, methanol and ethanol solvents with different dielectric constants (vacuum = 1, water = 78.39, methanol = 32.63, ethanol = 24.55) at three basis sets has shown a relatively change in geometrical parameters and stability energy. It is evident that transfer to a less polar solvent results a different shift.

Variation the relative energy versus dielectric constant is shown in Figure 2.

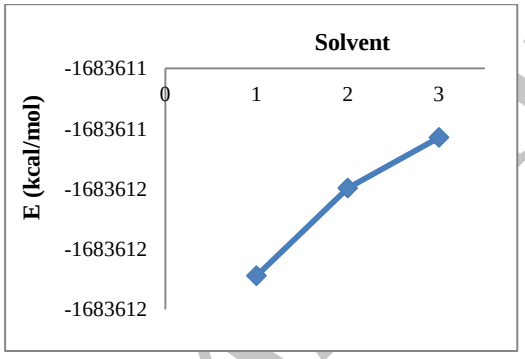

Figure 2. Stabilized energies (kcal/mol) of vinblastine versus different dielectric constants (1=water, 2=methanol and 3=ethanol solvents).

It is clear the energy of vinblastine changes in diverse media.

The energy of the drug was found to vary in studied solvents in the order water (-1683611.57 kcal mol-1) < methanol (-1683611.5 kcal mol-1) < ethanol (-1683611.46 kcal mol-1). Thus an increase in the dielectric constants increases the stability of vinblastine.

So the molecule is much stable in water media rather than the other solvents. As it is indicated in Table 1, dielectric constant has changed atomic charges. O29 and O30 have the most changes in atomic charge rather than the other atoms. O29 is more impressible by dielectric constant rather than O30. Bond lengths, bond angles and torsion angles are influenced by dielectric constant (Table 2). Variation of bond length (O29-O22), bond angle (O29-C22-O30) and torsion angle (O29-C22-O30-C35) versus dielectric constant are shown in Figure 3. The change in the bond angle and torsion angle is prominent by changing the solvent from methanol to ethanol and from water to vacuum, respectively (Figure 3).

The possible structures of vinblastine have been probed by stabilized energy. It was observed the trend of stability energies is as following: sto – 3 g > 3 - 21 g > 6 - 31 g basis sets by B3LYP method. Unlike the other solvents, it was observed that the change of energy in ethanol is different and increases from 3-21g to 6-31g basis set (Figure 4).

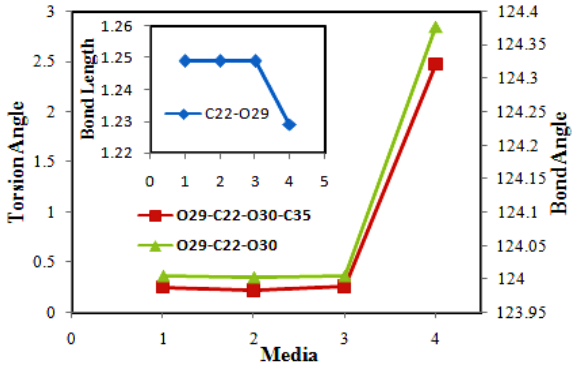

Figure 3. The curve of bond length (C22-O29), bond angle (O29-C22-O30) and torsion angle (O29-C22-O30-C35) versus different media (1=ethanol, 2=methanol, 3=water and 4= vacuum).

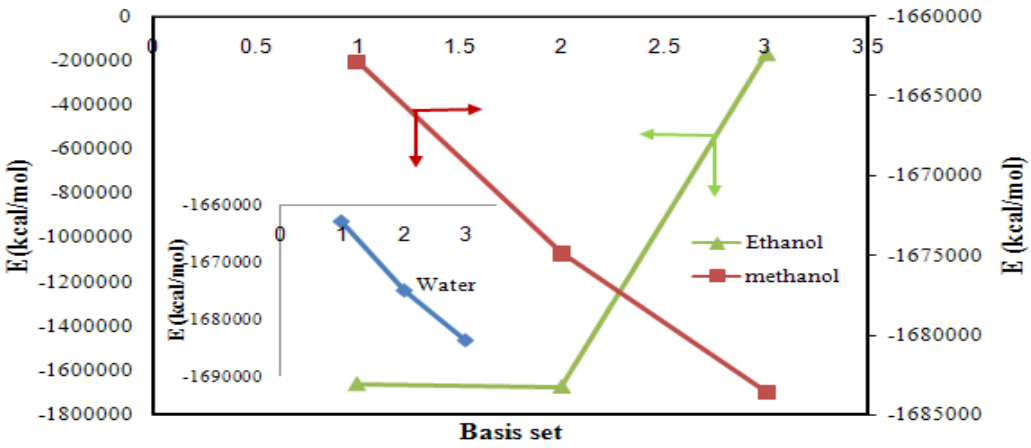

Figure 4. Stability energies of vinblastine versus basis sets (1= sto-3g, 2= 3-21g and 3= 6-31g) in different solvents.

The results of the above observations strongly suggest that the observed different curves are predominantly due to basis set functions and polarity of the environment.
Dramatic improvements in NMR shielding are observed in the NMR calculations on vinblastine using density functional theory (DFT).
In solvent effect studies, it is more advisable to carry out shielding calculations in solution even with a fixed (vacuum and liquid-phase optimized) solute geometry, than to perform shielding computations in vacuum for a solute where the geometry is optimized in solution.
The NMR measurements were carried out using B3LYP/sto-3g, 3-21g in CSGT methods of nuclear magnetic resonance in different dielectric constants (vacuum, water, methanol and ethanol) (Table 3).
The result of Table 3 shows the chemical shift (Δσ) of the vinblastine for each active atom (N12, N21, O29, O30, O43, O47 and N56). It was found that the O29 and O30 have maximal shift rather than other indicated atoms in all media (Figure 5). Values of chemical shift and chemical anisotropy have been decreased by increasing dielectric constant. Simulations and solvent NMR was performed by theoretical methods on vinblastine at various dielectric constants.

This paper is presented the theory and implementation of the Onsager model using density functional theory.
In this study, it is observed the small changes are seen in the reflect of NMR solvent effect theory.
Extrapolation schemes have significantly demonstrated that the O29 and O30 are the most active points at vinblastine, estimating the indicated structure-to-vacuum and liquid phases shift.
Therefore theoretical or computational steps are required to determine the properties of molecules, using solutions.

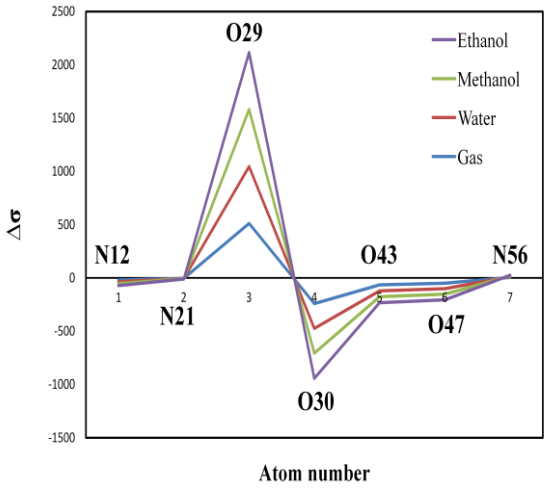

Figure 5. Plot of chemical shift (Δσ) versus atom numbers in different media.

Table 1. Atomic charges of vinblastine in different dielectric constant by HF and B3LYP methods.

	B3LYP								
1/ε	**1/78.39**			**1/32.63**			**1/24.55**		
Basis set	**Sto-3g**	**3-21g**	**6-31g**	**Sto-3g**	**3-21g**	**6-31g**	**Sto-3g**	**3-21g**	**6-31g**
C9	0.07288	0.37927	0.29361	0.07286	0.37922	0.29359	0.07285	0.3792	0.29348
N12	-0.2751	-0.8496	-0.80097	-0.2751	-0.84962	-0.80107	-0.2751	-0.84962	-0.80124
C13	0.06911	0.37163	0.26444	0.06904	0.37155	0.26433	0.06901	0.37154	0.26466
C15	-0.0941	-0.44224	-0.24196	-0.094	-0.44227	-0.24184	-0.094	-0.44241	-0.24189
C16	-0.05741	-0.17835	-0.09076	-0.05741	-0.17844	-0.09077	-0.0574	-0.17863	-0.09096
H17	0.22535	0.32453	0.32331	0.22525	0.32434	0.32307	0.22521	0.32422	0.32287
C20	-0.05433	-0.25382	-0.1445	-0.05432	-0.25383	-0.14445	-0.0543	-0.25381	-0.14425
N21	-0.24808	-0.54364	-0.49983	-0.24806	-0.54367	-0.50002	-0.2481	-0.54356	-0.50003
C22	0.21276	0.75569	0.5523	0.21276	0.75567	0.55229	0.21275	0.75563	0.5523
C27	-0.06637	-0.15278	-0.05536	-0.06638	-0.15282	-0.05527	-0.0664	-0.15294	-0.05573
C28	-0.07127	-0.17303	-0.09878	-0.07124	-0.17292	-0.09866	-0.0713	-0.17286	-0.09831
O29	-0.21766	-0.49864	-0.44477	-0.2161	-0.49854	-0.44468	-0.2176	-0.49848	-0.44476
O30	-0.17098	-0.50626	-0.50588	-0.17101	-0.50634	-0.50595	-0.171	-0.50645	-0.50589
C34	0.1006	0.14463	0.21441	0.1006	0.14454	0.21418	0.1006	0.14448	0.21483
C35	-0.12867	-0.34382	-0.17235	-0.12868	-0.34381	-0.17232	-0.1287	-0.34377	-0.17228
C37	0.05471	0.25789	0.23427	0.05467	0.25783	0.23423	0.05469	0.25768	0.23415
H40	0.06972	0.19793	0.12731	0.06972	0.19794	0.12723	0.06971	0.19802	0.12788
O43	-0.24749	-0.55025	-0.62845	-0.24746	-0.55011	-0.6283	-0.2474	-0.54981	-0.62831
C44	-0.1394	-0.35852	-0.22224	-0.13941	-0.35868	-0.2223	-0.1394	-0.35892	-0.22286
C45	0.05056	0.32461	0.25525	0.05051	0.32431	0.25467	0.05048	0.32415	0.25397
O47	-0.18746	-0.54791	-0.58192	-0.18741	-0.54783	-0.58182	-0.1874	-0.5477	-0.58195
C54	-0.22412	-0.57565	-0.4321	-0.22413	-0.5757	-0.43216	-0.2241	-0.57573	-0.43226
N56	-0.2339	-0.64373	-0.58545	-0.23395	-0.64354	-0.58509	-0.2339	-0.64329	-0.58453
H58	0.16916	0.33799	0.35591	0.16915	0.33787	0.35578	0.16914	0.33784	0.35567
	HF								
C9	0.10127	0.43472	0.35205	0.10125	0.43459	0.35207	0.10124	0.43466	0.35207
N12	-0.3265	-1.0342	-1.0382	-0.32654	-1.03408	-1.0382	-0.3266	-1.0342	-1.0383
C13	0.09723	0.42169	0.30436	0.09717	0.42149	0.30424	0.09714	0.42155	0.30419
C15	-0.065	-0.467	-0.2732	-0.06495	-0.46703	-0.2732	-0.0649	-0.467	-0.2732
C16	-0.01	-0.1211	-0.0533	-0.00999	-0.12146	-0.0534	-0.01	-0.1212	-0.0534
H17	0.21788	0.37057	0.38716	0.21781	0.37061	0.38702	0.21777	0.3703	0.38694
C20	-0.0272	-0.2335	-0.1376	-0.02718	-0.23368	-0.1375	-0.0272	-0.2334	-0.1375
N21	-0.2879	-0.7673	-0.7764	-0.2879	-0.76711	-0.7764	-0.2879	-0.7674	-0.7765
C22	0.31374	1.00246	0.83395	0.31372	1.0026	0.83389	0.31371	1.00242	0.83387
C27	-0.0239	-0.0757	0.00367	-0.02391	-0.07549	0.00363	-0.0239	-0.0757	0.00364
C28	-0.0282	-0.1262	-0.0483	-0.02823	-0.12639	-0.0482	-0.0282	-0.126	-0.0481
O29	-0.2665	-0.6348	-0.5884	-0.26644	-0.63507	-0.5884	-0.2664	-0.6347	-0.5884
O30	-0.2565	-0.7078	-0.7322	-0.25656	-0.70788	-0.7323	-0.2566	-0.7079	-0.7323
C34	0.14081	0.18004	0.2535	0.14081	0.17998	0.25345	0.14081	0.17999	0.25342
C35	-0.0634	-0.2815	-0.1237	-0.0634	-0.28146	-0.1237	-0.0634	-0.2815	-0.1236
C37	0.08919	0.38056	0.3989	0.08917	0.379	0.39874	0.08917	0.38037	0.39865
H40	0.04989	0.1933	0.15889	0.04989	0.19354	0.15887	0.04988	0.19325	0.15884
O43	-0.3018	-0.6949	-0.7814	-0.30174	-0.69479	-0.7813	-0.3017	-0.6948	-0.7813
C44	-0.1094	-0.3971	-0.277	-0.10937	-0.39693	-0.2773	-0.1094	-0.3973	-0.2774
C45	0.0601	0.35255	0.28682	0.06007	0.35018	0.28672	0.06005	0.35217	0.28667
O47	-0.2495	-0.7303	-0.8057	-0.24946	-0.73067	-0.8056	-0.2494	-0.7306	-0.8056
C54	-0.1861	-0.6103	-0.4812	-0.18605	-0.60988	-0.4812	-0.1861	-0.6103	-0.4812
N56	-0.2798	-0.8234	-0.813	-0.2798	-0.82114	-0.8129	-0.2798	-0.8232	-0.8129
H58	0.1705	0.37884	0.40304	0.17046	0.37861	0.40295	0.17044	0.37872	0.40291

Table 2. Bond lengths, bond angles and torsion angles of molecular geometry of vinblastine in different dielectric constants by HF and B3LYP methods.

	B3LYP								
1/ε	**1/78.39**			**1/32.63**			**1/24.55**		
Basis set	**Sto-3g**	**3-21g**	**6-31g**	**Sto-3g**	**3-21g**	**6-31g**	**Sto-3g**	**3-21g**	**6-31g**
C57-O47	1.486	1.495	1.480	1.486	1.495	1.480	1.486	1.495	1.480
H58-O43	1.027	0.994	0.978	1.027	0.994	0.978	1.027	0.994	0.978
C22-O30	1.432	1.373	1.375	1.432	1.373	1.375	1.432	1.373	1.375
C22-O29	1.249	1.229	1.236	1.249	1.229	1.236	1.249	1.229	1.236
O30-C35	1.481	1.479	1.472	1.481	1.479	1.472	1.481	1.479	1.472
N21-C28	1.523	1.485	1.473	1.523	1.485	1.473	1.523	1.485	1.473
H58-O43-C34	101.757	107.109	109.587	101.758	107.108	109.580	101.760	107.105	109.585
C45-C37-O47	118.744	120.130	120.697	118.754	120.121	120.692	118.745	120.109	120.697
C44-C34-O43	111.047	109.391	108.700	111.045	109.402	108.701	111.049	109.403	108.746
C34-C27-N21	114.432	113.327	111.437	114.439	113.330	111.421	114.433	113.371	111.504
O30-C22-O29	124.000	123.239	122.802	123.999	123.235	122.795	123.999	123.233	122.786
O29-C22-C15	127.490	126.436	126.130	127.486	126.441	126.133	127.489	126.444	126.130
C15-C22-O30	108.474	110.262	111.000	108.478	110.261	111.005	108.477	110.259	111.019
C15-C13-N12	118.146	118.838	117.433	118.146	118.837	117.442	118.139	118.833	117.498
C9-N12-C13	109.654	109.895	109.992	109.652	109.893	109.989	109.652	109.892	109.984
C9-N12-C13-C15	175.120	177.492	175.787	175.114	177.491	175.808	175.116	177.461	175.885
C16-N21-C27-C34	170.616	178.255	-177.152	170.597	178.263	-177.089	170.623	178.129	-177.226
H17-N12-C13-C15	0.976	0.922	0.464	1.034	0.934	0.445	1.024	0.943	0.385
C22-C15-C13-N12	-101.852	-112.367	-97.963	-101.838	-112.390	-98.097	0.943	-112.294	-98.720
C20-C15-C22-O30	-146.744	-146.474	-139.433	-146.721	-146.574	-139.452	-146.663	-146.712	-139.525
C28-N21-C27-C34	57.671	35.122	36.843	57.682	35.108	32.079	42.877	35.023	32.022
C35-O30-C22-O29	0.278	0.637	0.237	0.279	0.686	0.298	0.304	0.715	0.355
O43-C34-C27-N21	-159.820	-162.544	-173.605	-159.785	-162.494	-173.647	-159.807	-162.250	-173.184
C54-C44-C34-O43	65.584	61.914	58.157	65.571	61.973	58.155	65.583	62.053	58.001
N56-C45-C37-O47	5.138	-2.892	-2.283	5.126	-2.886	-2.288	5.112	-2.833	-2.270
H58-O43-C34-C27	-170.525	173.218	169.472	-170.485	173.490	169.671	-170.471	173.915	170.089
	HF								
C57-O47	1.442	1.469	1.455	1.442	1.469	1.455	1.442	1.469	1.455
H58-O43	0.989	0.966	0.951	0.989	0.966	0.951	0.989	0.966	0.951
C22-O30	1.396	1.346	1.343	1.396	1.346	1.343	1.396	1.346	1.343
C22-O29	1.214	1.206	1.214	1.214	1.206	1.214	1.214	1.206	1.214
O30-C35	1.437	1.453	1.447	1.437	1.453	1.447	1.437	1.453	1.447
N21-C28	1.488	1.466	1.459	1.488	1.466	1.459	1.488	1.466	1.459
H58-O43-C34	104.520	110.588	113.332	104.519	110.620	113.328	104.519	110.588	113.326
C45-C37-O47	121.813	120.589	120.697	121.806	120.564	120.689	121.805	120.579	120.686

C44-C34-O43	110.760	108.675	108.670	110.762	108.654	108.683	110.764	108.689	108.687
C34-C27-N21	112.650	110.811	112.032	112.653	110.789	112.037	112.650	110.812	112.041
O30-C22-O29	123.119	122.778	122.322	123.116	122.792	122.314	123.114	122.772	122.310
O29-C22-C15	127.194	126.359	125.768	127.199	126.369	125.779	127.202	126.365	125.784
C15-C22-O30	109.636	110.778	111.841	109.634	110.754	111.838	109.633	110.777	111.837
C15-C13-N12	116.189	118.579	117.048	116.187	118.575	118.575	116.183	118.582	117.050
C9-N12-C13	109.056	109.484	109.711	109.053	109.483	109.710	109.051	109.481	109.709
C9-N12-C13-C15	175.153	177.924	177.174	175.147	177.884	177.174	175.144	177.923	177.177
C16-N21-C27-C34	174.854	-175.377	-177.160	174.853	-175.361	-177.154	174.858	-175.348	-177.149
H17-N12-C13-C15	8.963	2.755	3.140	9.037	2.863	3.153	9.075	2.782	3.154
C22-C15-C13-N12	-86.631	-106.869	-98.840	-86.632	-106.838	-98.840	-86.614	-106.893	-98.861
C20-C15-C22-O30	-150.881	-152.377	-143.913	-150.942	-152.587	-144.005	-150.963	-152.493	-144.052
C28-N21-C27-C34	39.904	35.818	40.743	156.862	31.285	29.607	39.902	35.840	40.816
C35-O30-C22-O29	-0.008	-0.008	0.807	0.012	1.100	0.862	0.023	1.014	0.892
O43-C34-C27-N21	-171.990	-175.078	-169.354	-171.967	-175.239	-169.291	-171.977	-175.036	-169.260
C54-C44-C34-O43	57.908	54.018	57.433	57.920	54.022	57.460	57.925	54.052	57.470
N56-C45-C37-O47	3.201	-2.591	-3.266	3.199	-2.952	-3.288	3.198	-2.590	-3.294
H58-O43-C34-C27	176.844	163.718	171.045	176.885	163.414	171.283	176.901	163.954	171.386

Table 3. Values of NMR parameters of vinblastine interactions at indicated dielectric constants by B3LYP method at two basis sets using CSGT approximation.

1/ε		**Sto-3g**				**B3LYP / SCGT**	**3-21g**				
		σ_{iso}	**σ_{aniso}**	**η**	**δ**	**Δσ**	**σ_{iso}**	**σ_{aniso}**	**η**	**δ**	**Δσ**
1/00.00	N12	102.24	45.02	-0.40	-12.70	-19.05	121.86	60.88	-0.33	-15.63	-23.45
	N21	132.05	7.59	-1.98	-1.80	-2.70	213.60	32.74	-0.39	8.61	12.92
	O29	-133.88	512.73	0.14	340.81	511.21	-61.95	491.54	-0.20	325.30	487.96
	O30	20.15	136.30	0.08	-160.11	-240.17	99.97	138.53	0.09	-163.75	-245.62
	O43	72.40	50.73	0.27	-43.15	-64.73	166.13	51.48	0.86	-28.49	-42.74
	O47	86.79	92.08	-1.05	-32.82	-49.23	196.86	92.96	-2.81	-23.75	-35.63
	N56	112.69	24.03	-2.23	3.47	5.20	171.72	43.01	-0.50	13.91	20.87
1/78.39	N12	102.11	44.91	0.30	-11.42	-17.14	121.33	60.93	0.46	-13.68	-20.52
	N21	133.49	7.44	-2.77	-1.48	-2.22	214.16	32.32	-0.27	7.82	11.73
	O29	-167.11	549.08	0.36	356.28	534.42	-95.79	515.13	0.01	334.73	502.10
	O30	19.75	138.94	0.03	-155.45	-233.18	96.72	149.12	-0.09	-156.05	-234.08
	O43	78.13	62.97	0.53	-37.09	-55.63	170.92	44.81	0.81	28.99	43.49
	O47	90.64	85.10	-0.69	-34.39	-51.59	198.76	90.00	-2.93	-21.33	-32.00
	N56	115.86	25.86	-1.17	4.79	7.19	175.66	45.44	-0.20	14.86	22.29
1/32.63	N12	102.09	44.82	0.29	-11.39	-17.08	121.32	60.75	0.45	-13.60	-20.40
	N21	133.50	7.23	-2.73	-1.49	-2.24	214.24	32.22	-0.24	7.99	11.98
	O29	-167.68	549.31	0.36	356.48	534.72	-96.17	515.31	0.01	334.90	502.36
	O30	19.79	138.83	0.03	-155.58	-233.37	96.68	148.84	-0.09	-156.23	-234.35
	O43	77.80	63.03	0.51	-36.97	-55.46	170.75	44.04	0.83	28.53	42.79
	O47	91.30	84.42	-0.68	-34.46	-51.69	199.16	89.87	-2.94	-21.29	-31.94
	N56	115.83	25.92	-1.18	4.71	7.07	175.64	45.57	-0.20	14.78	22.17
1/24.55	N12	102.19	44.80	0.30	-11.60	-17.4052	121.39	60.79	0.46	-13.88	-20.82
	N21	133.39	7.39	-2.82	-1.46	-2.2039	214.13	32.29	-0.27	7.85	11.78
	O29	-167.83	549.63	0.35	356.91	535.3649	-96.06	515.24	0.01	335.14	502.71
	O30	19.84	138.92	0.02	-157.17	-235.762	96.70	148.86	-0.10	-157.75	-236.63
	O43	77.89	62.95	0.53	-37.07	-55.6101	170.66	44.76	0.80	29.02	43.53
	O47	91.23	84.88	-0.66	-34.37	-51.563	199.08	90.06	-2.96	-21.12	-31.69
	N56	115.71	25.67	-1.33	4.50	6.7513	175.56	45.33	-0.20	14.60	21.90

Conclusions

In this research, the vinblastine structure was optimized in vacuum and water, methanol and ethanol solvents, then the stability energy and structural properties such as bond lengths, bond angles, torsion angles and atom charges of the molecule were studied.

It was determined that the molecule is more stable in water rather than the other solvents and vacuum.

It was also specified that O29 and O30 are the most effective atoms of vinblastine, so this part of the molecule is active site of vinblastine that could bind to tubulin and perform the antimitosis and anticancer effects in process of cell division. The result of this research could use for studies of vinblastine binding to tubulin.

Acknowledgments

We acknowledge Department of Biology and Department of Chemistry in Islamic Azad University of Science and Research of Tehran.

Refrencess

1. Lobert S, Ingram JW, Correia JJ. The thermodynamics of vinca alkaloid-induced tubulin spirals formation. Biophys Chem. 2007; 126: 50-58.
2. Biswas BB, Sen K, Choudhury G, Bhattacharyya B. Molecular biology of tubulin: Its interaction with drugs and genomic organization. J Biosci. 1984; 6: 431-457.
3. Martin-Galiano AJ, Oliva MA, Sanz L, Bhattacharyya A, Serna M, Yebenes H, Valpuesta JM, Andreu JM. Bacterial tubulin distinct loop sequences and primitive assembly properties support its origin from a eukaryotic tubulin ancestor. Biol Chem. 2011; 286: 19789-19803.
4. Lobert S, Frankfuter A, Correia JJ. Energetics of vinca alkaloid interactions with tubulin isotypes: Implications for drug efficacy and toxicity. Cell Motil Cytoskel. 1998; 39: 107-121.
5. Mollaamin F, Varmaghani Z, Monajjemi M. Dielectric effect on thermodynamic properties in vinblastine by DFT/Onsager modelling. Phys Chem Liq. 2011; 49: 318-336.
6. Lobert S, Ingram JW, Hill BT, Correia JJ. A comparison of thermodynamic parameters for vinorelbine and vinflunine-induced tubulin self-association by sedimentation velocity. Mol Pharmacol. 1998; 53: 908-915.
7. Dong JG, Bornmann W, Nakanishi K, Berova N. Structural studies of vinblastine alkaloids by exciton coupled circular dichroism. Phytochemistry, 1995; 40: 1821-1824.
8. March NH, Knapp-Mohammady M. The inhomogeneous electron liquid in some bioinorganic assemblies studied by density functional methods. Phys Chem Liq. 2011; 49: 259-269.
9. Monajjemi M, Saeid L, Najafi F, Mollaamin F. Physical properties of active site of tubulin–binding as anticancer nanotechnology investigation. Int J Phys Sci. 2010; 5: 1609-1621.
10. Hehre WJ, Random L, Schleyer PVR, Pople JA. Ab initio molecular orbital theory. Wiley, New York; 1986.
11. Frisch MJ, Trucks GW, Schlegel HB, Scuseria GE, Robb MA, Cheeseman JR, et al. Gaussian 98. Revision A.7, Gaussian, Inc., Pittsburgh, PA; 1998.
12. Kanakaraju R, Kolandaivel P. Post Hartree–Fock and DFT studies on pyrrole···nitrogen and pyrrole···carbon monoxide molecules. Int j Mol Sci. 2002; 3: 777-789.
13. Lee C, Yang W, Parr GR. Development of the colle-salvetti correlation-energy formula into a functional of the electron density. Phys Rev. 1988; 37: 785-789.
14. Facelli JC (2002).Encyclopedia of Nuclear Magnetic Resonance; D. M.Grant, R. K. Harris, Eds., London: John Wiley & Sons. 9, 323-333.